Energy 211 (2020) 118570

Contents lists available at ScienceDirect

Energy

journal homepage: www.elsevier.com/locate/energy

Geometry definition and performance assessment of Tesla turbines for ORC

Lorenzo Talluri [a, *], Olivier Dumont [b], Giampaolo Manfrida [a], Vincent Lemort [b], Daniele Fiaschi [a]

[a] Department of Industrial Engineering, Università degli Studi di Firenze, Viale Morgagni 40-44, 50134, Firenze (FI), Italy
[b] Thermodynamics laboratory, Aerospace and Mechanical Engineering Department, University of Liège, Allée de la Découverte 17, 4000, Liège, Belgium

ARTICLE INFO

Article history:
Received 31 January 2020
Received in revised form
25 July 2020
Accepted 7 August 2020
Available online 15 August 2020

Keywords:
Tesla turbine
Fluid dynamics
ORC
Geometric definition

ABSTRACT

The Tesla turbine - also known as friction, viscous or bladeless turbine - is a peculiar expander, which generates power through viscous entrainment. In the last years, it has gained a renewed appeal due to the rising of distributed power generation applications. Indeed, this expander is not suitable to large size power generation, but it could become a breakthrough technology in the low power ranges, due to its characteristics of low cost and reliability. The current study presents a design approach to the Tesla turbine, applied to organic working fluids (R1233zd(E), R245fa, R1234yf, n-Hexane). Three fundamental geometric parameters are identified (rotor channel width/inlet diameter ratio, rotor outlet/inlet diameter ratio, throat width ratio) and their effects on the performance are analysed. The geometry of the turbine has been defined and the assessment of the performance potential is run, applying a 2D code for the viscous flow solution, considering real compressible fluid properties. For all the investigated working fluids, an efficiency higher than 60% has been achieved, with the defined geometry, under suitable thermo fluid-dynamic conditions.

1. Introduction

Alternative energy solutions for power generation are favoured by the strong commitment of the European Union to tackle climate change and by the limited fossil resources. Particularly, renewables, distributed energy conversion and heat recovery applications are being deeply investigated and developed, as they seem among the most suitable solutions able to fulfil the requirements for a cleaner future energy production.

In order to exploit the low temperature resources, which are typical of renewable energy resources and many waste heat sources from industrial processes or prime movers, the organic Rankine cycle power system (ORC) got the leadership, due to its favourable thermodynamic features coupled to a high degree of flexibility. ORC power system applications vary from heat recovery from gas turbines [1], internal combustion engines [2], or waste heat from industrial processes [3], to energy conversion from renewable resources (biomass [4], solar [5] or geothermal [6]). ORC power systems are also utilized for cogeneration of heat and power (CHP) [7]. In Ref. [8], an interesting market review is presented, where the principal applications, manufacturers, as well as market prediction of this technology are assessed.

The ORC power systems have several possibilities of optimization, which depend on the specific application. The optimization involves fluid selection as well as architecture configuration, both from a component and thermo/fluid-dynamics point of views. Micro-to-small scale ORCs usually utilize a basic configuration architecture, which includes a pump, an evaporator, an expander and a condenser. The most critical component for this kind of application is, generally, the expander, as it often does not meet the required characteristics of high efficiency, reliability, acceptable compactness and low costs.

Expanders for organic Rankine cycle are mainly divided in two categories: dynamic and volumetric expanders. Dynamic expanders are axial or radial turbines and are usually used for medium/high power applications (power achieved with radial turbines range from 50 to 500 kW; axial turbine show powers over 500 kW [9]). Volumetric types include a wide variety of expanders, such as scroll, screw, vane or piston, and are commonly utilized for small-micro power applications [10,11]. A complete description of

* Corresponding author.
E-mail address: lorenzo.talluri@unifi.it (L. Talluri).

https://doi.org/10.1016/j.energy.2020.118570
0360-5442/

expanders of different technologies is presented in Ref. [10], where geometrical and technical characteristics are reported. Moreover, a validated general semi-empirical approach is presented to model the performance of the volumetric expanders, while taking into account the relevant physical processes [10,11]. This model has been validated for different expanders technologies [11,12] and allows acceptable extrapolation characteristics [13]. Based on this model and on a literature review, it was shown that for small-scale organic Rankine cycles, there is no one specific optimal technology [11]. The best choice depends on the operating conditions of the application. Scroll expanders usually present the highest efficiency, piston solutions are attractive for high pressures and temperatures, root expanders are well fit to small pressure ratios (low temperature applications). The screw expanders present interesting part load performance through their wide range of shaft speeds, while the vane expanders show interesting efficiency in low temperature applications (<150 °C) [12]. Of course, other features such as handling of wet expansion, possibility of using an off-the-shelf compressor as expander [14], costs, availability, and power range must be taken into account in the final selection.

In recent years, a new expander for small-micro power application got an increasing interest in the scientific community, due to its characteristics of low-cost and reliability: The Tesla turbine. It is a bladeless turbine, composed by one or more nozzles that inject the working fluid tangentially inside the rotor. It is made of multiple stacked parallel disks; they are assembled very close to each other, forming very tight gaps, where the fluid exchanges work through viscous effects. The fluid enters from the periphery of the rotor and follows a spiral path before exiting through the rotor inner radius. The first concept of this turbine was developed by Tesla in 1913 [15]. Due to the advent of gas turbines and the run towards large size power plants in the following decades, as a result of the poor performance of this expander in high power applications, this technology did not find a commercial success and was not assessed until 1950. At that time, Leaman [16] investigated experimentally a 0.13 m rotor diameter turbine. Later some further research was carried out in the following years, especially by Rice, who developed an analytical solution and performed an extensive experimental test campaign on several Tesla turbine prototypes with air as working fluid [17]. But only in recent years, due to the renovated and growing interests towards distributed power generation, the research on the Tesla turbine has flourished. Of particular relevance are the studies carried out by Guha and Sengupta. In their work a comprehensive analytical model was developed and compared with computational fluid dynamics calculations [18]. The fluid dynamic behaviour of the flow inside the rotor and the contribution of each acting force were assessed. Another important line of research on Tesla turbines was performed by Carey, who developed an analytical model for the performance assessment of the expander [19]. Other relevant studies on Tesla turbines have dealt with analytical model development [20], performance assessment through the means of CFD [21] and experimental campaigns [22]. Particularly, Schosser et al. [23] performed an experimental campaign by the means of PIV measurements on an air driven Tesla turbine and compared the assessed velocity profile with numerical results.

In recent years, the application of the Tesla turbine for ORC was proposed by a number of researchers. Lampart and Jedrzejewski [24] developed an extensive CFD assessment on a 0.32 m rotor diameter, achieving 51% efficiency with a mass flow rate of 0.13 kg/s of Solkatherm SES36. Song et al. [25] developed an analytical model of Tesla turbines for ORC applications. The model was coupled with an ORC in order to assess the cycle performance. At design point, the ORC with R245ca released 1.25 kW power output with 4% thermodynamic cycle efficiency. In the following study Song et al. [26], improved the developed 1D model and compared the predicted performance with the experimental data obtained by Rice [17].

The most recent works on the Tesla turbine deal with the performance assessment, both through experimental campaigns [27,28], CFD analysis [29] or through the investigation of the possible utilization as heat recovery system from engine coolant waste heat [30].

The literature review shows that several analytical and numerical models were developed, and many experimental studies were carried out; but a clear and complete *geometry optimization and performance assessment of the Tesla turbine for ORC applications* seems to be still missing in literature. Indeed, the works dealing with the geometry optimization of the turbine are very few in literature [31–33] and most of them focus only on the rotor optimization with air or water as working fluids. In Ref. [31] the authors aim was to conceive a comprehensive model for the Tesla turbine working with organic fluids and not to develop scaling laws that can be applied in order to define the optimal configuration. In Ref. [32], a rotor optimization procedure was developed through the application of CFD analysis considering water as working fluid. The main assessed parameters were the gap and the number of disks. In Ref. [33], similarity scaling laws were formulated for the rotor of a Tesla turbine. Seven non dimensional parameters were defined, including both geometric and fluid-dynamic non dimensional numbers, through the application of the Buckingham Pi theorem. The validity of the similitude analysis was demonstrated through the development of CFD analysis with air as working fluid. Therefore, the main goal of this study is to develop geometric scaling laws which enable the definition of the correct geometry of the turbine, as function of the external rotor diameter and to conduct a performance assessment of the optimized design with various organic working fluids. Particularly, 4 workings fluids have been analysed in this work: R1233zd(E), R245fa, R1234yf, n-Hexane. R245fa is considered as reference in literature, because as hydrocarbons substitute it allows to achieve the best efficiency levels. R1234yf and R1233zd(E) are selected because they represent the new generation of organic fluids with low environmental impact (replacing respectively R134a and R245fa). N-Hexane is on the other hand adopted as reference hydrocarbon, due to its favourable thermodynamic critical conditions (particularly, by the low critical pressure when compared to refrigerants). The analysis is carried out for all fluids at a fixed total inlet temperature of 100 °C and total inlet pressure corresponding to a 10 °C super heating level in order to compare all the different investigated fluids at the same low temperature level.

2. Methodology

2.1. Tesla turbine model

The Tesla turbine 2D thermo-fluid dynamics model was developed in Engineering Equation Solver (EES) environment [34]. The software is a common equation-solving program, which however, has a major advantage having a high accuracy thermodynamic property database, which includes hundreds of working fluids. The developed model therefore exploits the real fluid properties included in the EES thermodynamic database and, thus, allows calculation of density and viscosity – as well as all the other thermodynamic functions – as function of local variables (typically pressure and temperature). Particularly, the fluids properties applied are expressed in terms of the reduced Helmholtz energy, usually with the density and temperature as independent variables [35–38].

The Tesla turbine 2D code has been explained in detail and

validated against other models in the technical literature and through numerical computations in Refs. [20,31]. The complete set of equations can be found in Ref. [31], but it is also concisely reported in annex A. Particularly, the validation was performed through the comparison of the obtained results by the code and the 2D, 3D and experimental data available in literature, especially when air was utilized as working fluid. The code was also validated against experimental results obtained with R1223zd(E) as working fluid, showing a very good match, especially if the turbine blockage, windage and pumping losses were considered [39]. Particularly, it was found that the code reliability for low pressure cases (e.g. air as working fluid) is very good (within 2%), while when high pressure conditions are analysed (e.g. organic working fluids), the strong influence of blockage, windage and pumping losses increases the uncertainty of the model to a value of 15%. However, if the actual mechanical issues (e.g. leakage around the rotor) could be avoided, the expected uncertainty would fall within the range of low pressure conditions, therefore between 2 and 5%. Here, for the sake of brevity, only the fundamental reduced Navier-Stokes equations in cylindrical coordinates are reported. Equation (1) is the reduced θ-Momentum equation and Eq. (2) is the reduced r-Momentum equation, which allow to calculate the gradient of relative tangential velocity and static pressure in radial direction.

$$\frac{\partial w_\theta}{\partial r} = -\frac{10}{a}\Omega - \left(\frac{60\nu}{w_r a b^2} + \frac{1}{r}\right)\cdot w_\theta \tag{1}$$

$$\frac{1}{\rho}\frac{dp}{dr} = -w_r\frac{\partial w_r}{\partial r}\cdot\frac{a^2}{30} + \Omega^2 r + 2\Omega w_\theta\frac{a}{6} + \frac{w_\theta^2}{r}\cdot\frac{a^2}{30} - \nu w_r\cdot\frac{2a}{b^2} \tag{2}$$

The "a" coefficient takes into account the variation of the fluid behaviour inside the channel, assuming low value (around 4) for the entry region and high values (6–8) for fully developed flow as suggested in Ref. [40]. The model was applied systematically in the present study, determining the velocity, pressure and temperature profiles along the rotor. A stator nozzle/bladed passage model was added, including the estimation of losses due to partial admission [41]. The application of the model also allows calculating mass-averaged values of power and efficiency, which are the fundamental performance parameters investigated for each design condition here examined. Indeed, the developed model has been exploited in order to develop geometry correlations which could be utilized for the definition of the optimal geometry of the turbine.

2.2. Definition of geometry

Similarity scaling laws concepts are applied in order to perform the sizing of the turbine. Therefore, all the principal geometric parameters were analysed with the goal of maximizing the turbine total-to-total efficiency; nonetheless, for the sake of brevity only the three parameters that affect the performance of the turbine the most are here assessed. The scaling laws are developed in order to link every geometric parameter to the external rotor diameter.

The main parameters analysed in this work are reported in the following:

- Rotor channel width/inlet diameter ratio ($B = b/D_2$);
- Rotor outlet/inlet diameter ratio ($R = D_3/D_2$);
- Throat/width ratio ($TWR = \frac{TW*H_s*Z}{\pi*D_2*b*n}$).

The first two ratios are very well-known optimization parameters, as highlighted in literature [18], while the third one has been found to be critical when dealing with the complete optimization of the turbine, therefore taking into account not only the rotor, but also the stator. The assessment of each parameter directly linked to the external rotor diameter allows to immediately understand the volume of the expander.

Furthermore, stator inlet/outlet diameter ratio is fixed at 1.25. This value is assumed as suggested in Ref. [42], while the gap dimension was chosen as small as possible, compatibly with the thermal expansion of the disks. Fig. 1 displays the scheme and Table 1 reports the main nomenclature of the assessed Tesla turbine configuration. In the following subsections, each parameter will be assessed in order to understand its influence on the performance of the turbine. Afterwards, the fluid dynamic conditions are considered, in order to identify the critical parameters that affect the power and efficiency of the turbine.

2.2.1. Rotor channel width/inlet diameter

The non-dimensional rotor channel width is function of the external rotor diameter, which was calculated by means of an extensive parametric analysis. Fig. 2a shows the total-to-total efficiency of the turbine vs. channel width, at fixed 100 °C total inlet temperature and total inlet pressure corresponding to a 10 °C super heating level (or, in other words, a pressure corresponding to a 90 °C saturation temperature). This choice has been made in order to assess all the different investigated fluids at the same low temperature level, however, it will not impact on the results, as the performance of the turbine is not directly affected by the thermodynamic conditions, but to the obtained velocities (Mach number). For the sake of clarity, Fig. 2a shows the results for a fixed 0.2 throat Mach number and a 0.4 rotor outlet/inlet diameter ratio. The throat/width ratio (TWR) is fixed at 0.02 at 100 °C temperature. The parametric analysis was performed at various throat Mach numbers (0.2, 0.3, 0.6, 0.9) to assess if compressibility effects (from almost incompressible to almost sonic flow) would change the optimizing R value; different rotor diameter ratios (R = 0.2, 0.4, 0.6) and throat/width ratios (0.02, 0.04). The effect of throat Mach number, R and TWR do not remarkably influence the position of the best efficiency, but only its value (Fig. 2a). Fig. 2b shows the loci of best efficiency ($\eta_{TT} = \frac{W}{\Delta h_{0ss}} = \frac{v_{\theta 2}u_2 - v_{\theta 3}u_3}{(h_{00} - h_{03ss})}$) achieved by interpolation of the non-dimensional rotor channel width as a function of rotor outlet diameter at highest efficiency. The quadratic interpolated equation for the determination of the non-dimensional rotor channel width B, which allows achieving the highest efficiency vs. rotor outer diameter D_2 is reported in Eq. (3) for R1233zd(E) (equations for different fluids are presented and discussed in the results section).

$$B = 0.0021*D_2^2 - 0.0017*D_2 + 0.0006 \tag{3}$$

2.2.2. Rotor outlet/inlet diameters

The best conditions for the rotor outlet/inlet diameter ratio (R) are evaluated running several parametric analyses (determining different Mach number conditions). It is found that when the optimal non-dimensional channel width correlation (reported in the previous section) is applied, the best value for practically every turbine size is always in the range 0.3–0.4, with the lower bound corresponding to low Mach number (0.2–0.3) and the higher limit to high Mach number (close to 1). Fig. 3 displays the total-to-total efficiency as a function of R for different Ma (0.2, 0.3, 0.6 and 0.9), referring to the lower (0.08 m) and upper (0.44 m) diameter range limits considered in this analysis. Smaller turbines can achieve higher efficiency at the price of a lower power production and higher rotational speeds. In the present analysis, a value of R = 0.35 is selected, which guarantees good efficiencies for all the

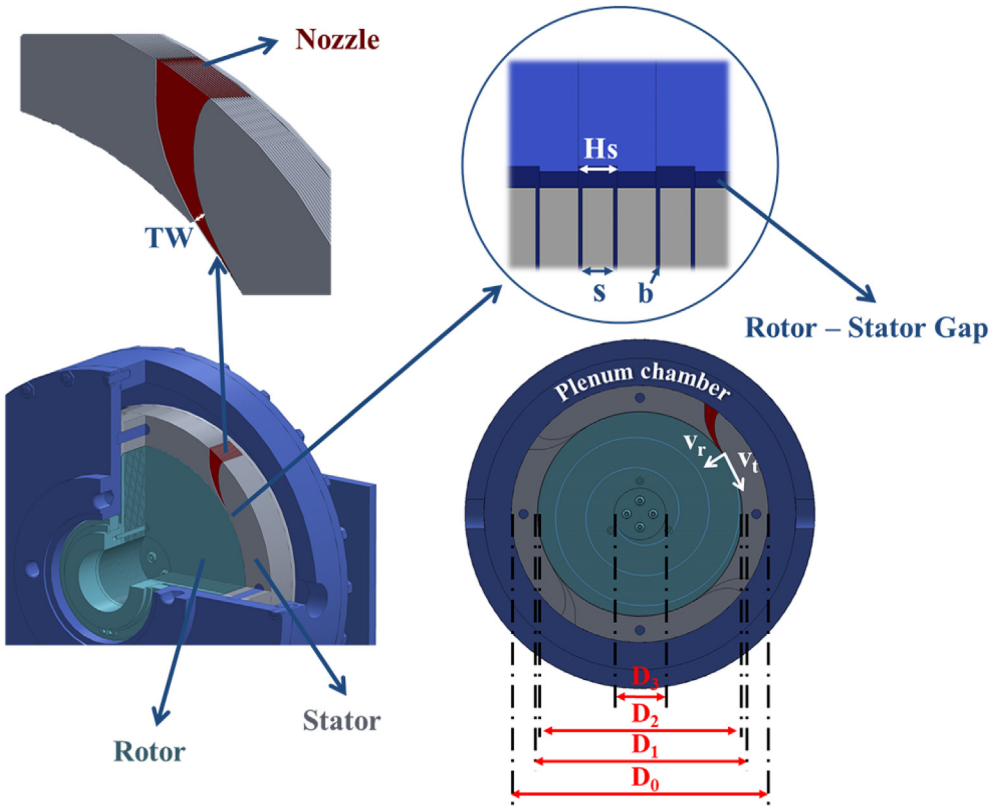

Fig. 1. Schematic of Tesla turbine.

Table 1
Turbine geometry.

Component	Parameter	Symbol
Stator	Stator inlet diameter	D_0
	Stator outlet diameter	D_1
	Nozzle throat height	Hs
	Nozzle throat width	TW
Rotor	Rotor inlet diameter	D_2
	Rotor outlet diameter	D_3
	Channel height	b
	Disks thickness	s

investigated Mach numbers.

2.2.3. Throat/width

The throat-width ratio is determined as the ratio between stator outlet area and rotor inlet area, as defined by Eq. (4):

$$TWR = \frac{TW*H_s*Z}{\pi*D_2*b*n} \quad (4)$$

It was found that the total-to-total efficiency increases linearly with decreasing TWR. Actually, low TWRs imply higher velocities at the throat, which are beneficial for rotor efficiency. On the other hand, the power output shows an opposite behaviour, steadily increasing with increasing TWR. Therefore, a balanced solution was adopted, that is, TWR = 0.02. The balanced solution takes into account both thermodynamic matters (high efficiency at a suitable power) and manufacturing issues: in fact, selecting low TWRs implies manufacturing of very small stator channels, which must respect a precise geometry, which is crucial for achieving the very high required value of the outlet angle (typically, 85–87°). This can be noted in Fig. 4, where the efficiency and the single nozzle throat area have been shown. The area of the single nozzle drastically drops lowering the TWR. It is important not to pursue the lowest value of TWR (which could give the highest efficiency), because it would result in an increase of the manufacturing complexity of the piece, which would be in countertendency with the expander aim (low cost). Indeed, a very low TWR would certainly increase the efficiency, but would require a large expander (increasing of D_2 at denominator of Eq. (4)).

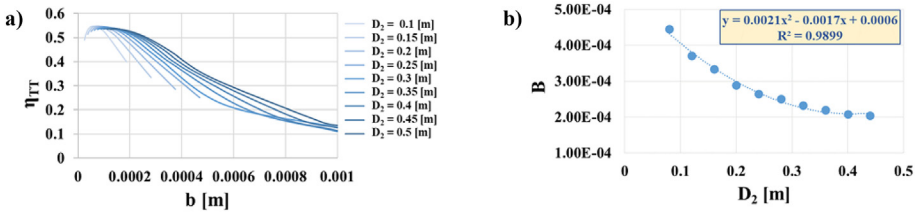

Fig. 2. a) Total-to-total efficiency against channel width; b) Quadratic interpolation of non-dimensional channel width against rotor external diameter at highest efficiency value.

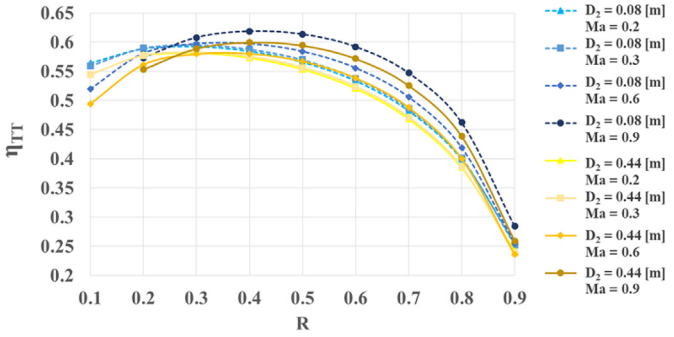

Fig. 3. Total-to-total efficiency against rotor outlet/inlet diameter ratio R.

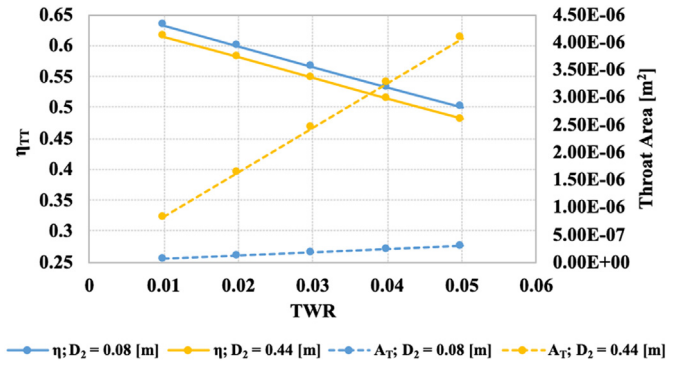

Fig. 4. Total-to-total efficiency and throat area against throat width ratio TWR.

2.3. Fluid dynamics assessment

Following the definition of the main geometric parameters, a fluid dynamics assessment was performed in order to achieve best efficiencies. The assessment was carried out varying the throat Mach number at stator outlet (and consequently mass flow rate) and the tangential velocity ratio $\sigma = \frac{v_{t2}}{u_2}$ at rotor inlet.

Once the geometry assessment is carried out, increasing throat Mach number allows an improvement of both efficiency and power. The increase in efficiency is moderate, whereas the power increase is quite relevant. The tangential velocity ratio σ is one of the most important parameters for Tesla turbine optimization. The right matching of rotor inlet tangential velocity and peripheral speed is of paramount importance to achieve a high efficiency. In practise, the total-to-total efficiency is at its highest at $\sigma = 1$, or very close to 1 (Fig. 5). This is due to the correct value of the inlet tangential relative velocity in this condition, which must be close to zero. At higher values of σ, the fluid-machine work transfer would not be optimal, as the absolute velocity drops drastically at rotor inlet, dissipated into heat and not usefully transmitted to the rotor by the viscous forces. On the other hand, if a value lower than 1 is considered, a reversal flow conditions is triggered. In fact, if the absolute tangential velocity is lower than the rotational speed, a negative relative tangential velocity results at rotor inlet, so that the turbine would behave as a compressor at least in rotor entry region. However, values lower than 1, but close to unity may be considered to achieve high efficiency levels. Indeed, if the flow reversal region is very limited, the higher power produced by the remaining inner region of the rotor, operating at a higher rotational speed while keeping all other parameters unchanged, counterbalances the negative effect of the flow reversal. As a result, the best values of the tangential velocity ratio σ are found in the range 0.9–1.

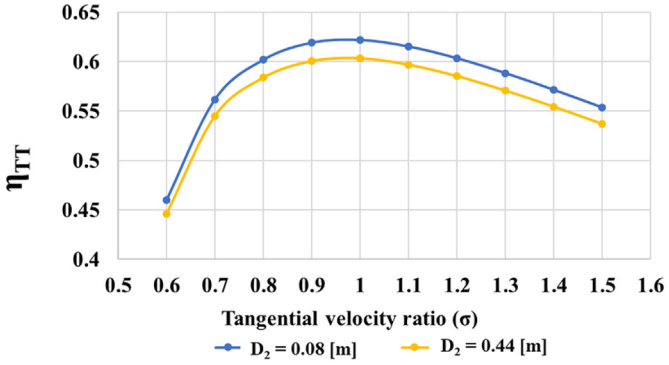

Fig. 5. Total-to-total efficiency tangential velocity ratio for two different Tesla turbine sizes.

2.4. Compact design

As discussed in the previous section, the right matching between inlet tangential velocity in the rotor and rotational speed is of paramount importance to achieve high turbine performances. In order to have the proper match, the rotational speed needs to be adapted to the rotor external diameter. Specifically, the smaller the rotor, the higher the rotational speed required for best efficiency (Fig. 6). The machine compactness is another fundamental parameter, depending on the specific requirements of the field of application, and is clearly related to the rotational speed. For example - referring to expanders in the power range from 1 to 30 kW - for the automotive sector, compactness is a fundamental parameter, and therefore a small, fast-turning Tesla turbine would be preferable; on the other hand, for domestic applications, the Tesla concept offers – with respect to other possible expanders, such as centripetal turbines - the attractive possibility of direct coupling with a 3000 rpm generator and a low noise emission factor; for these applications compactness of the machine could be sacrificed.

The compactness factor CF is the ratio between the power and the total volume of the turbine, expressed in kW/m^3 [11]; the calculated values of CF are shown together with the rotational speed as a function of the rotor size in Fig. 5, where $T_{00} = 100$ °C, $P_{00} = 833{,}000$ Pa and mass flow rates between 0.08 and 1.1 kg/s are considered.

3. Results

3.1. Assessment of geometry

Considering different working fluids, the obtained geometry as a

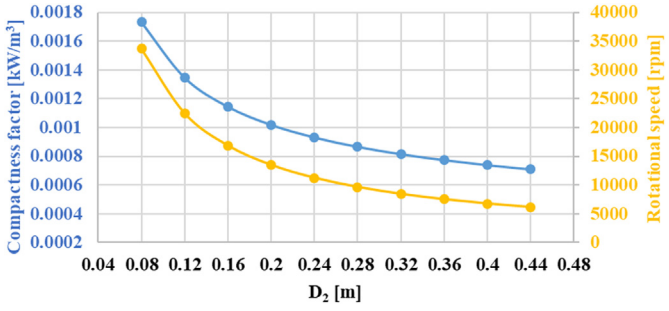

Fig. 6. Compactness factor CF and rotational speed for assessed Tesla turbine geometry ($Ma_1 = 1$; $\sigma = 10.08 < D_2 < 0.44$ m).

function of rotor outer diameter results to be optimized within similar ranges of the main design parameters; the rotor outlet/inlet diameter ratio lies between $0.3 < R < 0.4$, the throat width ratio is about $TWR = 0.02$, and the throat Mach number Ma and tangential velocity ratio σ should be close to unity; however, the main parameter which must be adapted to different fluids is the non-dimensional rotor channel width B (Table 2). Referring to ORC applications of the Tesla turbine, even if an optimal value of b can be found for each working fluid, values around 0.0001 m are required in order to obtain high efficiency. Lower rotor channel width values are beneficial for refrigerants, and especially for fluids with low critical temperature and high critical pressure (such as R1234yf). Conversely, hydrocarbon fluids such has n-Hexane, allow higher rotor channel width, because of their low critical pressure and high critical temperature, which are opposite to those of refrigerants. Furthermore, it was verified for all examined working fluids that high values of the tangential velocity ratio σ correspond to a not proper work transfer between the fluid and the rotor; on the other hand, values lower than 1 imply a reverse flow region at inlet.

When constrained rotational velocity applications are considered, high expander efficiencies are directly related to a proper selection of the rotor diameter. Indeed, as shown in Fig. 7, fixing the rotational speed implies assuming an inlet tangential velocity ratio (for fixed thermodynamic conditions); therefore, as stated in the previous section, both expansion ratio β and efficiency are maximised when σ approaches unity.

3.2. Efficiency versus power and expansion ratio

The most suitable range of the design expansion ratio for the Tesla turbine should be between 3.5 and 5.5, depending on the working fluid (Fig. 8). The power range, which depends on the number of channels of the turbine, can be between a few Watts and 30–35 kW (considering configurations in a range from 2 to 100 rotor channels). At high expansion ratios, the turbine is subject to large pressure losses, thus undergoing an efficiency penalty, mainly due to the stator - rotor gap loss and to the high kinetic energy loss at expander outlet. Fig. 7 displays the total-to-total efficiency of a 100-channels Tesla turbine as a function of power and expansion ratio. It is important to notice that the maximum efficiency level is almost the same for all the considered fluids (between 0.609 and 0.626). The expansion ratio determining best efficiency values is similar for all fluids, but shows some sensitivity to the different fluid characteristics (slightly higher values for refrigerants, slightly lower for hydrocarbons). R1233zd(E) and R245fa (very similar fluids in terms of thermodynamic properties) hold the same optimizing range of expansion ratio, i.e. between 4 and 5. On the other hand, R1234yf requires higher pressures at the same temperature level, hence it shows optimal conditions between 3 and 4. Conversely, n-Hexane, achieving the lowest efficiency at the fixed 100 °C temperature level, requires higher expansion ratios, between 4.5 and 6. Furthermore, best efficiency conditions are achieved at low power output, especially in the case of hydrocarbon fluids.

Table 2
Calculated values of rotor channels width for the investigated fluids.

Fluid	Non-dimensional rotor channel width (B)
R1233zd(E)	$B = 0.0021 * D_2^2 - 0.0017 * D_2 + 0.0006$
R245fa	$B = 0.0025 * D_2^2 - 0.002 * D_2 + 0.0006$
R1234yf	$B = 0.0008 * D_2^2 - 0.0007 * D_2 + 0.0003$
n-Hexane	$B = 0.0047 * D_2^2 - 0.0039 * D_2 + 0.0013$

3.3. Compactness and power output (optimized speed)

Fig. 9 displays the behaviour of the compactness factor [11]. This is a fundamental indicator when selecting a micro-expander. As can be noted from Fig. 8, the Tesla turbine can be quite bulky ($CF < 10^{-3}$) when large rotor diameters are considered, especially for fluids with low pressure levels such as n-Hexane (Fig. 8d). On the other hand, it can become compact ($CF > 1.5 \cdot 10^{-3}$) when high power production is accomplished using refrigerant fluids under high-pressure conditions (such as R1234yf, Fig. 8c). Indeed, high-pressure conditions mean that the mass flow rate through the turbine is higher and, consequently, the power output increases. Therefore, a compact turbine utilizing a refrigerant can be suggested for applications where the compactness of the expander is the most important parameter, such as in the automotive field. Fig. 8 shows also the power range for each considered fluid as a function of rotor diameter and number of channels. The throat Mach number was fixed at 1 in order to achieve the maximum possible expansion ratio. The right compromise between compactness and power production depends on the selected fluid, but rotor diameters between 0.16 and 0.24 m can be recommended to guarantee a compact machine with reasonable power output levels. It should be remarked that high-pressure inlet conditions, as for R1234yf, allow combining a relevant power output and a compact expander (almost 30 kW with $CF > 1.3 \cdot 10^{-3}$). Comparing the values of CF with those typical of volumetric expanders [11], it appears that the Tesla turbine may be in the same range of roots and piston, and close to scroll expanders. Nonetheless, it would certainly be always bulkier than screw expanders, which achieve a very high value of CF (up to $2.0 \cdot 10^{-2}$).

4. Conclusions

A design approach for Tesla turbine was applied in order to evaluate the performance with different possible working fluids for ORC applications.

The assessment of the turbine power range, as a function of geometric and thermodynamic parameters, was the pivotal point of this research. The key outcomes are summarised in the following:

- Geometric sizing guidelines are proposed to achieve high performance of Tesla turbine working with 4 different fluids.
- The most critical parameters for achieving good turbine performance are found to be the rotor inlet tangential velocity ratio σ, the non-dimensional rotor channel width B and the rotor outlet/inlet diameter ratio R. Reference values for each fluid are provided within the considered power range (0.05 kW–30 kW). The recommended value for the non-dimensional rotor channel width is a quadratic function of rotor inlet diameter and the rotor outlet/inlet diameter ratio should be between 0.3 and 0.4.
- Proper design expansion ratios for the Tesla turbine are determined between 3.5 and 5.5. This range of expansion ratios is quite common in low temperature applications, which may be considered, therefore, to be the optimal field of application of this turbine.

Hydrocarbon fluids are suitable for micro power generation. Specifically, n-Hexane achieves high efficiency at low-pressure levels. Nonetheless, if a high power per unit volume is required, organic refrigerants appear to be a good choice, as the power output per channel is definitely higher when compared to hydrocarbons.

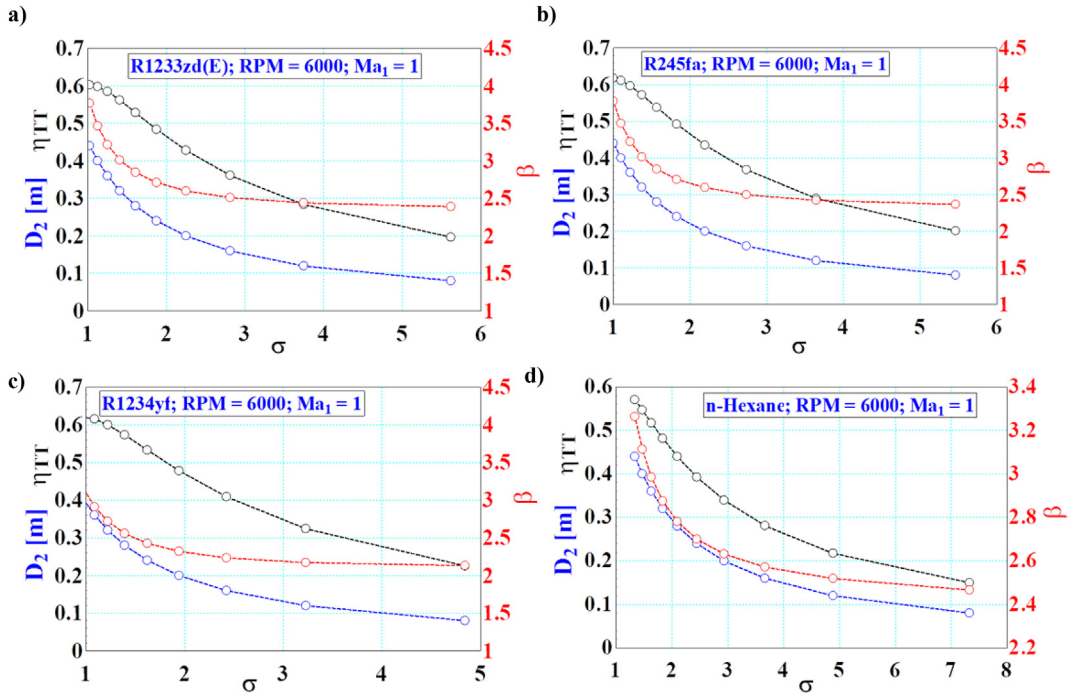

Fig. 7. Tangential velocity ratio, efficiency and expansion ratio at a fixed 6000 RPM rotational speed ($Ma_1 = 10.08 < D_2 < 0.44$m).

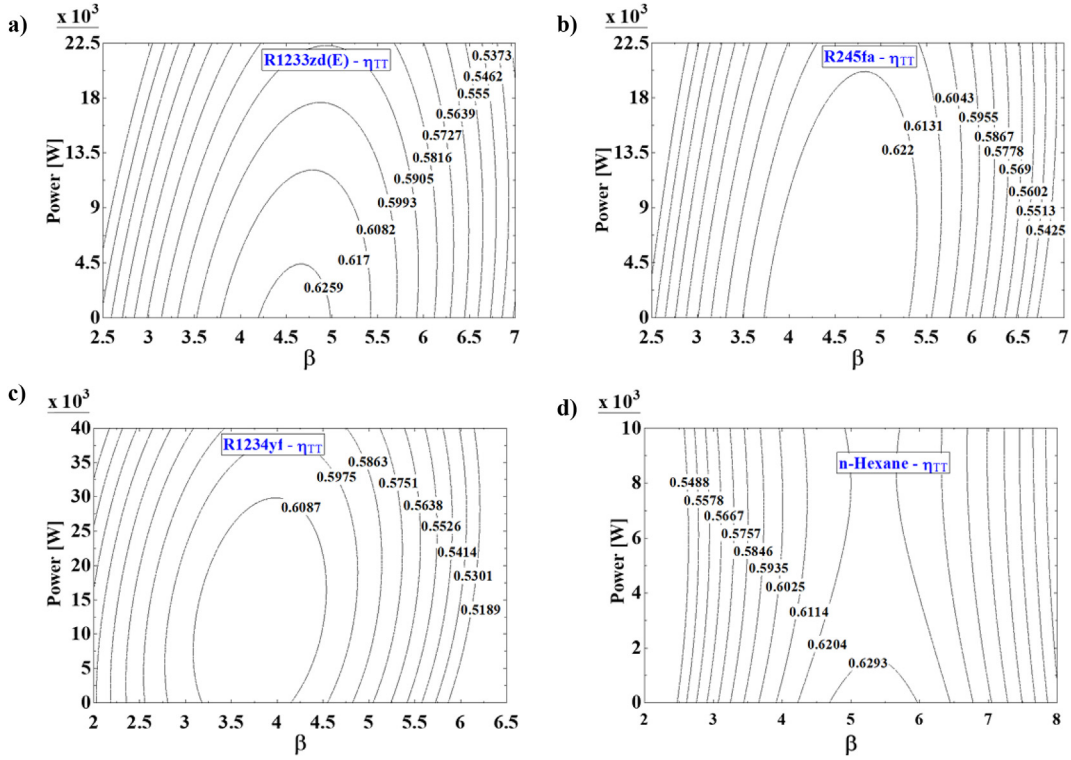

Fig. 8. Efficiency vs of power output and expansion ratio for a) R1233zd(E), b) R245fa, c) R1234yf; d) n-Hexane ($Ma_1 = 1$; $0.9 < \sigma < 2.250.08 < D_2 < 0.44$ m, $n_{TOT} = 100$).

Credit author statement

Lorenzo Talluri: Investigation, Methodology, Software, Writing-Original draft preparation, Writing- Reviewing and Editing. Olivier Dumont: Investigation, Methodology, Writing- Reviewing and Editing. Giampaolo Manfrida: Supervision, Conceptualization, Writing- Reviewing and Editing. Vincent Lemort: Supervision, Conceptualization, Writing- Reviewing and Editing. Daniele

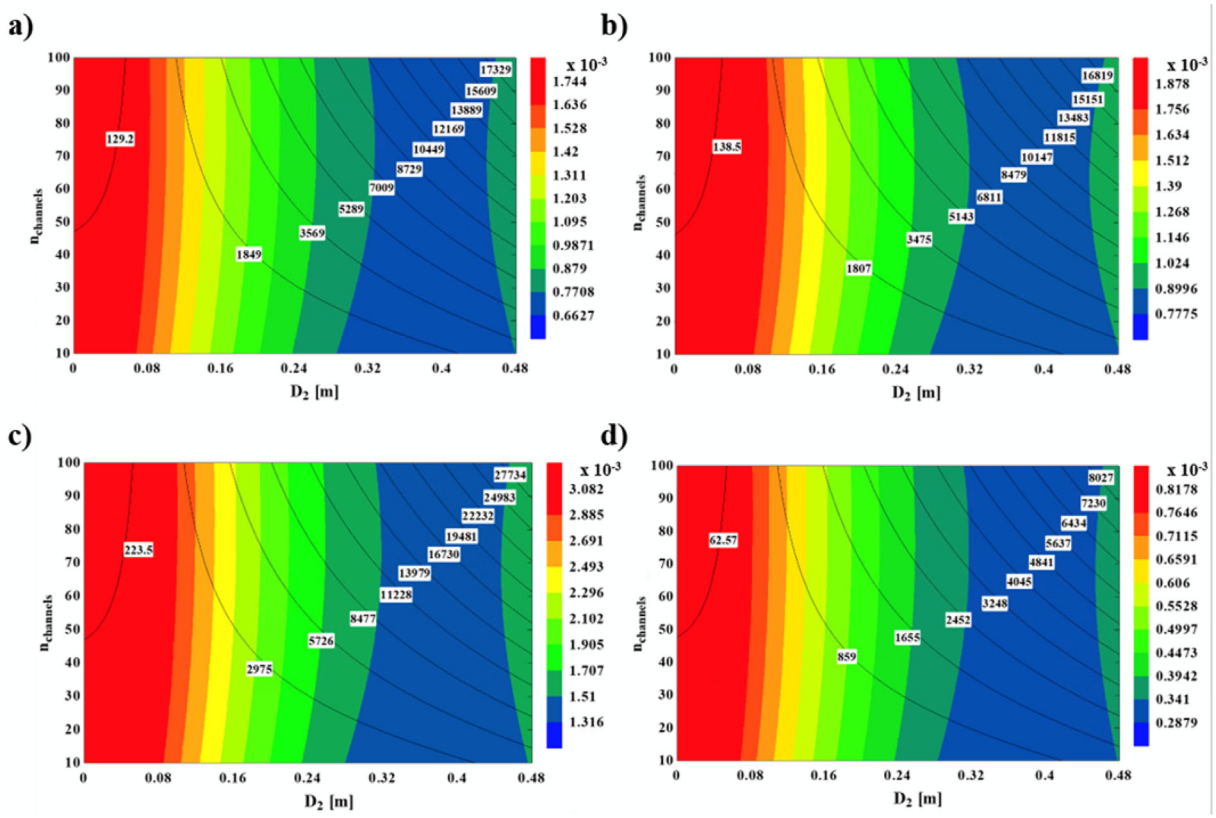

Fig. 9. Compactness (colour legend) and power output (black lines on the graphs with corresponding caption) as function of turbine size, channel and rotor diameter, for a) R1233zd(E), b) R245fa, c) R1234yf; d) n-Hexane ($Ma_1 = 1$; $\sigma = 1$). (For interpretation of the references to colour in this figure legend, the reader is referred to the Web version of this article.)

Fiaschi: Supervision, Conceptualization, Writing- Reviewing and Editing.

Declaration of competing interest

The authors declare that they have no known competing financial interests or personal relationships that could have appeared to influence the work reported in this paper.

Nomenclature

a	Coefficient
A_T	Throat area (m^2)
b	Rotor channel width (m)
B	Rotor channel width/inlet diameter
CF	Compactness factor (kW/m^3)
D	Diameter (m)
h	Specific enthalpy (kJ/kg)
H_s	Stator height (m)
n	Number of rotor disks per stator disk
n_{TOT}	Total number of rotor disks
p	Pressure (Pa)
r	Radius (m)
R	Rotor Inlet/Outlet diameter ratio
s	Disk thickness (m)
TW	Throat width (m)
TWR	Throat width ratio
u	Rotational velocity (m/s)
v	Absolute velocity (m/s)
w	Relative velocity (m/s)
W	Specific work (kJ/kg)
Z	Number of nozzles per stator disk

Greek symbols

β	Expansion ratio
η_{TT}	Total-to-total efficiency
ν	Kinematic viscosity (m^2/s)
ρ	Density (kg/m^3)
σ	Tangential velocity ratio at rotor inlet
Ω	Rotational speed (rad/s)

Subscripts and superscripts

0, 1, 2, …	Reference point of expander sections
0	Total conditions
r	Radial direction
ss	Isentropic
θ	Tangential direction

Annex A. Rotor thermo-fluid dynamic model

Assumptions

Steady state, laminar, viscous, and two dimensional flow; the body forces were assumed negligible.

Following [18], the Navier-Stokes equations were reduced to:

Continuity equation:

$$\frac{1}{r}\frac{\partial(rw_r)}{\partial r} = 0 \tag{A.1}$$

r-Momentum equation:

$$w_r\frac{\partial w_r}{\partial r}-\Omega^2 r-2\Omega w_\theta-\frac{w_\theta^2}{r}=-\frac{1}{\rho}\frac{dp}{dr}+\nu\frac{\partial^2 w_r}{\partial^2 z} \quad (A.2)$$

θ-Momentum equation:

$$w_r\frac{\partial w_\theta}{\partial r}+\frac{w_r w_\theta}{r}+2\Omega w_r=\nu\frac{\partial^2 w_\theta}{\partial^2 z} \quad (A.3)$$

z-Momentum equation:

$$\frac{\partial p}{\partial z}=0 \quad (A.4)$$

The model introduces an axial velocity profile, so that the relative velocities in r and θ directions may be expressed as:

$$w_\theta(r,z)=\overline{w}_{\theta 2}\zeta(R)G(z) \quad (A.5)$$

$$w_r(r,z)=\overline{w}_{r2}\xi(R)H(z) \quad (A.6)$$

where:

$$R=\frac{r}{r_2};\ \zeta(R)=\frac{\overline{w}_\theta(r)}{\overline{w}_{\theta 2}};\ \xi(R)=\frac{\overline{w}_r(r)}{\overline{w}_{r2}};$$

$$G(z)=\frac{w_\theta(r,z)}{\overline{w}_\theta(r)};\ H(z)=\frac{w_r(r,z)}{\overline{w}_r(r)}$$

G(z) and H(z) are the variations of tangential and radial velocities respectively along z direction.

Following the procedure outlined in [18], it was assumed that the velocity profile of the fully developed flow was laminar, thus parabolic. Furthermore, in order to generalize the mathematical model of the flow, a coefficient for the parabolic velocity profile was defined. Accordingly, G(z) and H(z) can be expressed as:

$$G(z)=H(z)=a\frac{z}{b}\left(1-\frac{z}{b}\right)=a\frac{z}{b}-a\left(\frac{z}{b}\right)^2 \quad (A.7)$$

and

$$w_r(r,z)=\overline{w}_r\cdot 6\frac{z}{b}\left(1-\frac{z}{b}\right) \quad (A.8)$$

$$w_\theta(r,z)=\overline{w}_\theta\cdot 6\frac{z}{b}\left(1-\frac{z}{b}\right) \quad (A.9)$$

Integrating the differential form of the θ-momentum and r-momentum equations between z = 0 and z = b/2, and applying the boundary conditions reported in [18], which assumed maximum velocity value at mid channel and zero velocity at the walls, it was possible to calculate the gradient of relative tangential velocity and static pressure in radial direction.

$$\frac{\partial w_\theta}{\partial r}=-\frac{10}{a}\Omega-\left(\frac{60\nu}{w_r a b^2}+\frac{1}{r}\right)\cdot w_\theta \quad (A.10)$$

$$\frac{1}{\rho}\frac{dp}{dr}=-w_r\frac{\partial w_r}{\partial r}\cdot\frac{a^2}{30}+\Omega^2 r+2\Omega w_\theta\frac{a}{6}+\frac{w_\theta^2}{r}\cdot\frac{a^2}{30}-\nu w_r\cdot\frac{2a}{b^2} \quad (A.11)$$

The rotor model was completed with the mass balance, which allows the calculation of the radial velocity:

$$V_r=-\frac{\dot{m}}{2\pi r b\rho} \quad (A.12)$$

Equation (A.10 and A.11) were numerically solved by applying a step forward method (Centered Finite Difference): the rotor channel was discretized in radial direction with a predefined number of equal steps.

Finally, the rothalpy conservation (eq. A.13) was applied to calculate the local value of static enthalpy:

$$h=I_2-\frac{w^2}{2}+\frac{u^2}{2} \quad (A.13)$$

References

[1] Invernizzi C, Iora P, Silva P. Bottoming micro-Rankine cycles for micro-gas turbines. Appl Therm Eng 2007;27:100–10.
[2] Vaja I, Gambarotta A. Internal combustion engine (ICE) bottoming with organic rankine cycles (ORCs). Energy 2010;35:1084–93.
[3] Desideri A, Gusev S, Van Den Broek M, Lemort V, Quoilin S. Experimental comparison of organic fluids for low temperature ORC (organic Rankine cycle) systems for waste heat recovery applications. Energy 2016;97:460–9.
[4] Schuster A, Karellas S, Kakaras E, Spliethoff H. Energetic and economic investigation of organic rankine cycle applications. Appl Therm Eng 2009;29:1809–17.
[5] Zhai H, Dai YJ, Wu JY, Wang RZ. Energy and exergy analyses on a novel hybrid solar heating, cooling and power generation system for remote areas. Appl Energy 2009;86:1395–404.
[6] Fiaschi D, Manfrida G, Rogai E, Talluri L. Exergoeconomic analysis and comparison between ORC and Kalina cycles to exploit low and medium-temperature heat from two geothermal sites. Energy Convers Manag 2017;154:503–16.
[7] Tempesti D, Manfrida G, Fiaschi D. Thermodynamic analysis of two micro CHP systems operating with geothermal and solar energy. Appl Energy 2012;97:609–17.
[8] Tartière T, Astolfi M. A word overview of the organic rankine cycle market. In: Energy procedia, vol. 129; 2017. p. 2–9.
[9] Talluri L, Lombardi G. Simulation and design tool for ORC axial turbine stage. In: Energy procedia, vol. 129; 2017. p. 277–84.
[10] Lemort V., Legros A., Positive displacement expanders for organic rankine cycle systems, in: Macchi M. and Astolfi M., Organic rankine cycle (ORC) power systems, technologies and applications, first ed., Woodhead Publishing, Elsevier.
[11] Dumont O, Parthoens A, Dickes R, Lemort V. Experimental investigation and optimal performance assessment of four volumetric expanders (scroll, screw, piston and roots) tested in a small–scale organic Rankine cycle system. Energy 2018;165:1119–27.
[12] Guillaume L. On the design of waste heat recovery organic Rankine cycle systems for engines of long-haul trucks. PhD thesis. University of Liège; 2017.
[13] Dumont O, Dickes R, Lemort V. Extrapolability and limitations of a semi-empirical model for the simulation of volumetric expanders. Energy Procedia 2017;129:315–22.
[14] Dumont O, Quoilin S, Lemort V. Experimental investigation of a Scroll unit used as a compressor and as an expander in a Heat Pump/ORC reversible unit. In: International refrigeration and air conditioning conference, Purdue; 2014.
[15] Tesla N., 1913, Turbine, U.S. Patent No. 1 061 206.
[16] Leaman AB. The design, construction and investigation of a Tesla turbine. University of Maryland; 1950. M.Sc. Thesis.
[17] Rice W. An analytical and experimental investigation of multiple-disk turbines. J Eng Power Trans ASME 1965;87:29–36.
[18] Guha A, Sengupta S. The fluid dynamics of work transfer in the non–uniform viscous rotating flow within a Tesla disc turbomachine. Phys Fluids 2014;26:1–27.
[19] Carey VP. Assessment of Tesla turbine performance for small scale rankine combined heat and power systems. J Eng Gas Turbines Power 2010;132:1–8.
[20] Manfrida G, Talluri L. Fluid dynamics assessment of the Tesla turbine rotor. Therm Sci 2019;23:1–10.
[21] Choon TW, Rahman AA, Jer FS, Aik LE. Optimization of Tesla turbine using computational fluid dynamics approach. In: IEEE Symposium on Industrial Electronics and Applications (ISIEA2011); 2011.
[22] Neckel AL, Godinho M. Influence of geometry on the efficiency of convergent–divergent nozzles applied to Tesla turbines. Exp Therm Fluid Sci 2015;62:131–40.
[23] Schosser C, Lecheler S, Pfizner M. A test rig for the investigation of the performance and flow field of Tesla friction turbines. In: Proceedings of ASME turbo expo 2014: turbine technical conference and exposition; 2014 [Dusseldorf].
[24] Lampart P, Jedrzejewski L. Investigations of aerodynamics of Tesla bladeless microturbines. J Theor Appl Mech 2011;49(2):477–99.
[25] Song J, Gu CW, Li XS. Performance estimation of Tesla turbine applied in small scale Organic Rankine Cycle (ORC) system. Appl Therm Eng 2017;110:318–26.

[26] Song J, Ren XD, Li XS, Gu CW, Zhang MM. One dimensional model analysis and performance assessment of Tesla turbine. Appl Therm Eng 2018;134:546–54.
[27] Placco GM, Guimaraes LNF. Power analysis on a 70-mm rotor Tesla turbine. J Energy Resour Technol 2019;142(3):031202.
[28] Renuke A, Traverso A, Pascenti M. Experimental campaign testes on a Tesla micro-expander. In: E3S Web Conf. – SUPER19 SUstainable PolyEnergy generation and HaRvesting, 113; 2019, 03015.
[29] Renuke A, Traverso A, Pascenti M. Performance assessment of bladeless micro-expanders using 3D Numerical simulation. In: E3S Web Conf. – SUPER19 SUstainable PolyEnergy generation and HaRvesting, 113; 2019, 03016.
[30] Ji F, Bao Y, Zhou Y, Du F, Zhu H, Zhao S, Li G, Zhu X, Ding S. Investigation on performance and implementation of Tesla turbine in engine waste heat recovery. Energy Convers Manag 2019;179:326–38.
[31] Talluri L, Fiaschi D, Neri G, Ciappi L. Design and optimization of a Tesla turbine for ORC applications. Appl Energy 2018;226:300–19.
[32] Choon TW, Rahman AA, Her FS, Aik LE. Optimization of Tesla turbine using Computational Fluid Dynamics approach. In: IEEE Symposium on Industrial Electronics and Applications, Langkawi; 2011. p. 477–80.
[33] Guha A, Sengupta S. Similitude and scaling laws for rotating flow between concentric discs. In: Proceedings of the institution of mechanical engineers, Part A. Journal of Power and Energy; 2014.
[34] Klein SA, Nellis GF. Mastering EES. f-Chart software; 2012.
[35] Mondejar ME, McLinden MO, Lemmon EW. Thermodynamic properties of trans-1-chloro-3,3,3-trifluoropropene (R1233zd(E)): vapor pressure, p-rho-T data, speed of sound measurements and equation of state. J Chem Eng Data 2015;60:2477–89.
[36] Eric W. Lemmon, roland span "short fundamental equations of state for 20 industrial fluids". J Chem Eng Data 2006;51(3):785–850.
[37] Richter Markus, McLinden Mark O, Lemmon Eric W. Thermodynamic properties of 2,3,3,3-Tetrafluoroprop-1-ene (R1234yf): vapor pressure and p-rho-T measurements and an equation of state. J Chem Eng Data 2011;56:3254–64.
[38] Span R, Wagner W. Equations of state for technical applications: II results for non-polar fluids. Int J Thermophys Jan. 2003;24(No. 1).
[39] Talluri L, Dumont O, Manfrida G, Lemort V, Fiaschi D. Experimental investigation of an organic rankine cycle Tesla turbine working with R1233zd(E). Appl Therm Eng 2020;174.
[40] Ciappi L, Fiaschi D, Niknam PH, Talluri L. Computational investigation of the flow inside a Tesla turbine rotor. Energy 2019;173:207–17.
[41] Manfrida G, Pacini L, Talluri L. An upgraded Tesla turbine concept for ORC applications. Energy 2018;158:33–40.
[42] Glassman AJ. Computer program for design analysis of radial-inflow turbines. Technical report. National Aeronautics and Space Administration; 1976.